COMPARATIVE MOLECULAR DOCKING STUDIES OF ISOQUINOLINE FUSED BICYLES WITH JANUS KINASE PROTEINS

Dissertation submitted to the University of Kerala in partial fulfilment of the requirement for the award of the Degree of Master of Science in Chemistry

M.Sc. CHEMISTRY

2020-2022

CONTENTS

ABSTRACT

Janus kinase gene plays major role in cell growth and proliferation by making JAK1, JAK2, JAK3 and TYK2 proteins which are a part of JAK/STAT signalling pathway, which transmits chemical signals from outside the cell to its nucleus. Janus Kinase mutation leads to certain disorders such as; Rheumatoid arthritis, Psoriasis, Ulcerative colitis, Crohn disease, Polycythaemia Vera (PV), Myeloproliferative Neoplasm (MPN), Primary and secondary Myelofibrosis; Acute Myeloid Leukaemia (AML), Essential Thrombocythemia etc. MPN is accompanied by inflammation, splenomegaly and thrombosis. Janus Kinase inhibitors were developed to treat these diseases. Isoquinoline and its derivatives possess various therapeutic activities which includes anti-tumor, anti-bacterial, anti-malerial, anti-inflammatory, anti-viral, antimicrobial and so on. Medicinal chemists are depending on CADD as an efficient way of identifying a potential lead compound and designing powerful drugs for treating disorders. Molecular docking analysis performed on JAK1 (3EYG), JAK2 (3FUP), JAK3 (5LWM) and TYK2 (4GJ2) of Janus Kinase protein using auto dock. The difference in binding energy obtained is noted. The ligand which obtained least binding energy with these Janus Kinase proteins can be further modified as their respective inhibitor drugs by enriching their potential.

CHAPTER 1

INTRODUCTION

1.1. JANUS KINASE

JAKs appear to be the primary signalling mediators activated by cytokines that employ these receptors since they constitutively bind the membrane-proximal domains of Type I and II cytokine receptors. JAK1, JAK2, JAK3, and TYK2 are the four mammalian orthologs of this tiny but evolutionarily conserved family, which also includes teleosts, birds, and insects.[1] JAK1, JAK2, JAK3, and TYK2 are members of the Janus kinase (JAK) family of non-receptor protein-tyrosine kinases (tyrosine kinase-2). A JAK homology pseudokinase (JH2) domain is found in each of these proteins, and it controls the nearby protein kinase domain (JH1). JAK3 is mostly found in hematopoietic cells, whereas JAK1/2 and TYK2 are expressed everywhere. Numerous cytokines, including as interleukins, interferons, and hormones like erythropoietin, thrombopoietin, and growth hormone, regulate the Janus kinase family. When a ligand binds to cytokine and hormone receptors, it activates the corresponding Janus kinases, which then cause the receptors to be phosphorylated. Signal transducers and activators of transcription (STATs) connect to the receptor phosphotyrosines through their SH2 domain, which encourages STAT phosphorylation by Janus kinases and subsequent activation. The translocation of STAT dimers to the nucleus allows them to participate in the control of the expression of several proteins. Autoimmune diseases like rheumatoid arthritis, ulcerative colitis, and Crohn's disease are brought on by JAK-STAT dysregulation. The development of myelofibrosis, polycythemia vera, and other myeloproliferative diseases is also

influenced by JAK-STAT dysregulation. A lesser number of patients with various neoplasms and 95% of those with polycythemia vera have the activating JAK2 V617F mutation. While JAK1/2 signalling plays a role in the pathogenesis of numerous malignancies, such as leukemias, lymphomas, and myeloproliferative neoplasms, JAK1/3 signalling plays a role in the pathogenesis of inflammatory diseases. The FDA has given the pan-JAK inhibitor tofacitinib and the JAK1/2 inhibitor ruxolitinib approval to treat rheumatoid arthritis, polycythemia vera, and myelofibrosis, respectively.[2]

1.1.1. JAK1

A human tyrosine kinase protein called JAK1 is required for certain type I and type II cytokines to signal. It interacts with the common gamma chain (γc) of type I cytokine receptors to elicit signals from the gp130 receptor family (including the IL-6R, IL-11R, LIF-R, OSM-R, cardiotrophin-1 receptor (CT-1R), ciliary neurotrophic factor receptor (CNTF-R), neurotrophin-1 receptor (NNT-1R), and leptin-R) as well as the IL-2 receptor family (including It is crucial for type II cytokine receptors, type I (IFN-α/β) and type II (IFN-γ) interferons, and members of the IL-10 family to transmit a signal.[1] Individual cancer cells can contract when JAK1 is expressed, which may help them escape their tumour and spread to other regions of the body.[3]

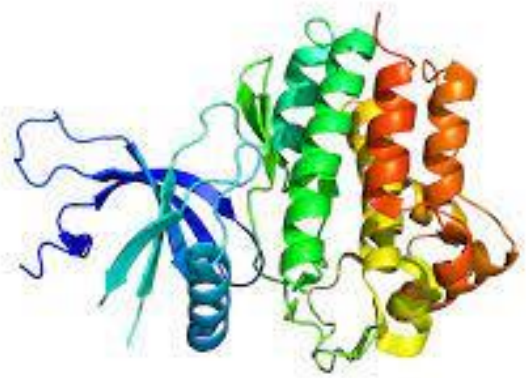

Figure 1: Structure of **JAK1**

1.1.2. JAK2

JAK2 gene make a protein that send signals to promote cell growth and helps to control the number of red blood cells, white blood cells and platelets that are made in bone marrow. JAK2 is located on chromosome 9p24 and includes 25 exons. Its protein has 1132 amino acids and pervasively expressed in mammalian cells. JAK-STAT signalling play crucial role in cellular processes, survival and normal functioning of hematopoietic, immune, cardiac cells.[4]

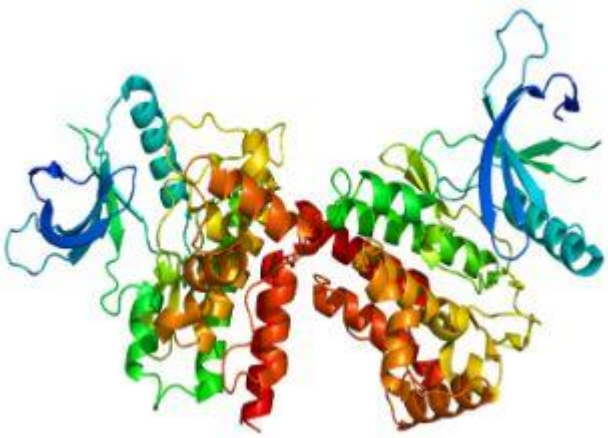

Figure 2: Structure of **JAK2**

1.1.3. JAK3

Cytosolic tyrosine kinase JAK3 is particularly linked to cytokine receptors. JAKs are necessary for cytokine receptor proteins to start signalling when their ligands are bound because they lack enzymatic activity (e.g. cytokines). Based on their various domains and activation motifs, the cytokine receptors can be grouped into five primary classes. The type I receptors that use the common gamma chain (γc) need JAK3 to signal. According to studies, JAK3 is crucial for immunological and non-immune cell physiology. Epithelial-mesenchymal transition, cell survival, proliferation, development, and differentiation are all regulated by epithelial JAK3.[5] JAK3's function in cytokine signalling is expected to be more constrained than that of other JAKs because it is expressed in hematopoietic and epithelial cells. Although it has been discovered in intestinal epithelial cells[6,7,8], it is most frequently expressed in T cells and NK cells.[9] The type I cytokine receptor family's common gamma chain (c)-using receptors use JAK3 to transmit signals (e.g. IL-2R, IL-4R, IL-7R, IL-9R, IL-15R, and IL-21R).[10]

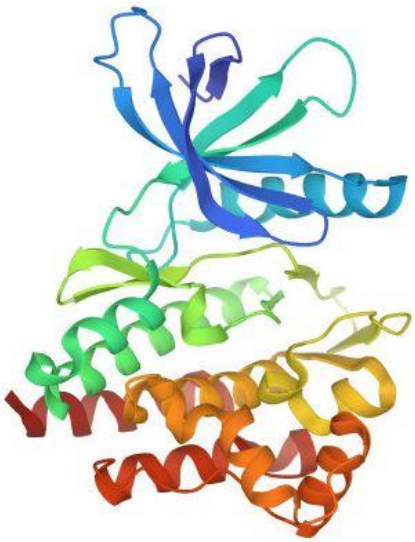

Figure 3: Structure of **JAK3**

1.1.4. TYK2

Tyrosine-protein Kinase TYK2 is a non-receptor enzyme in human encoded as TYK2 gene.[11] TYK2 was the first JAK family member to be described (the other members are JAK1, JAK2, and JAK3).[12] It has been implicated to the signalling of IFN-α, IL-6, IL-10, and IL-12. On the basis of research of murine models, which show that TYK2 operates largely in IL-12 and type I-IFN signalling, TYK2 has more extensive and profound activities in humans than previously recognised. Human cells are more severely affected by TYK2 deficiency than mouse cells are. TYK2 has significant influence on the transduction of IL-23, IL-10, and IL-6 signals, in addition to IFN- and - and IL-12 signalling. Since a broad family of cytokines, including IL-6, IL-11, IL-27, IL-31, oncostatin M (OSM), ciliary neurotrophic factor, cardiotrophin 1, cardiotrophin-like cytokine, and LIF, all signal through the same gp-130 receptor-chain, TYK2 may also impact signalling through these cytokines. TYK2 activation by IL-12 and IL-23 is shared by their ligand and receptor subunits, which has recently come to light. TYK2 is activated by IL-10, and its deficiency hinders generation and response to IL-10.[13]

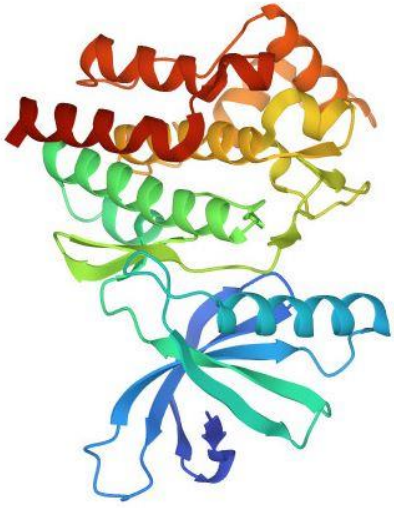

Figure 4: Structure of **TYK2**

1.2. JAK Mutation and Related Diseases

JAK mutation can cause inflammatory and neoplastic disorders. It contributes to inflammatory diseases such as Rheumatoid arthritis, Psoriasis, Ulcerative colitis, Crohn disease and neoplastic diseases such as Myelofibrosis, Polycythemia vera, Primary thrombocythemia.[2]

AML, ALL, breast ductal carcinoma, and NSCLC are caused by somatic mutations in the SH2 domain and the small and large lobes of the pseudokinase domain of JAK1.[14] T-cell ALL activating mutation incidence ranges from 6 to 27%, while B-cell ALL activating mutation incidence is at 1.5% and T-cell prolymphocytic leukaemia activating mutation incidence is from 8 to 12%.[2] While mutations in the small lobe of the pseudokinase domain have been found in both ALL and polycythemia vera, more than thirty JAK2 mutations in exon 12 (^{535}MVFHKIRNEDLIF^{547}) cause polycythemia vera.[14] The R683 residue, which is near the end of the β7′-strand below the ATP-binding site of JH2 and may interact with the β2-β3 loop of the small lobe of JH1, is the site of the bulk of JAK2 mutations in lymphoid lineage neoplasms. Acute megakaryoblastic leukaemia (15%) has been linked to mutations in the JAK3 pseudokinase N-lobe, while breast ductal carcinomas and ALL are linked to mutations in the large lobe. About 21% of T-cell ALL have been reported to contain TYK2 mutations.[2] Multiple TYK2 variants demonstrate a substantial association with autoimmune diseases like multiple sclerosis, systemic lupus erythematosus, Crohn disease, primary biliary cirrhosis, and type I diabetes. TYK2 deficits are linked to vulnerability to viral and bacterial infections. Additionally, TYK2 polymorphisms have been associated to AML.

Rare chromosomal rearrangements connecting the oligomerization domains of either TEL, BCR, PCM1, Pax5, or ETV6 to the JH1 domain coding part of the JAK2 gene have been observed in atypical acute myelogenous leukemia. JAK2 JH1 activation and subsequent downstream signalling via the STAT, phosphatidylinositol 3-kinase, or MAP kinase pathways are caused by the fusion proteins' oligomerization and promotion of the transphosphorylation of the activation regions. And in some B-cell lymphomas as well as 30–50% of Hodgkin lymphomas, the JAK2 locus is amplified.[2]

1.3. JAK Inhibitors

JAK inhibitors, sometimes referred to as jakinibs or Janus kinase inhibitors, are a class of drugs that block the activity of one or more members of the Janus kinase family of enzymes (JAK1, JAK2, JAK3, or TYK2), hence disrupting the JAK-STAT signalling pathway. These inhibitors can be used therapeutically to treat inflammatory conditions like rheumatoid arthritis and cancer.[15,16,17] Their application to treat various skin conditions is of interest.[18] Since JAK3 functions are primarily limited to lymphocytes, it is appealing as a potential treatment for a variety of autoimmune disorders. As of 2017, research and development for a selective JAK3 inhibitor are ongoing.[19] Janus kinase inhibitors fall under the categories of immunomodulators, disease-modifying antirheumatic medicines (DMARDs), and tyrosine kinase inhibitors, many of which overlap. They alter the immune system by inhibiting cytokine function. Cytokines are essential for regulating immune response and cell proliferation. Many cytokines bind to and activate type I and type II cytokine receptors in order to function. For the purpose of signal transduction, these receptors in turn rely on the Janus kinase (JAK) family of enzymes. Therefore, drugs that inhibit these Janus

kinases from hindering cytokine signalling.[15] Janus kinases preferentially phosphorylate cytokine receptors that have been activated. By attracting STAT transcription factors, these phosphorylated receptors in turn modulate gene transcription.[20] Tofacitinib was the first JAK inhibitor to reach clinical trials. Tofacitinib is a highly selective inhibitor of JAK3 (IC_{50} = 2 nM), which prevents IL-2, IL-4, IL-15, and IL-21 from acting. Tofacitinib works to treat allergy disorders by preventing the differentiation of Th2 cells. In a lesser degree, tofacitinib inhibits JAK1 (IC_{50} = 100 nM) and JAK2 (IC_{50} = 20 nM), which prevents IFN-γ and IL-6 signalling and, as a result, T_h1 cell differentiation.[15] One mechanism (related to psoriasis) is that IL-17 and the harm it produces are diminished when Jak-dependent IL-23 is blocked.[18]

1.4. Role of Isoqunoline fused bicycles

Isoquinoline alkaloids, a significant class of N-based heterocyclic chemicals, have drawn study interest from all over the world since the early 19th century due to their diverse bioactivities. Antitumor, anti-diabetic, antibacterial, antiviral, anti-fungal, anti-parasitic, anti-inflammatory, antioxidant, and neuroprotective effects are some of these bioactivities. Isoquinoline alkaloids can be used to create potent medications. Some well-known medications made from isoquinoline include the analgesic Morphine, the antibiotic Berberine, the antitussive Codeine, the antirheumatic Sinominone, and the acetyl cholinesterase inhibitor galanthamine. Over the past 200 years, isoquinoline has been the subject of thousands of books, papers, and other publications, proving its superiority as a drug discovery tool. There are simple isoquinoline alkaloids as Benzyl and Aporphine. Neferine is a form of bisbenzylisoquinoline alkaloid with sedative, antiarrhythmic, antihypertensive,

relaxant, and anti-diabetic properties. Berberine extracted from rhizome roots also has myocardial protective effects and antitumor, anti-inflammatory, antibacterial, and antiviral properties.[21] Corydalis hendersonii Hemsl (CH), a traditional Tibetan medicine, is essential in the management of high-altitude polycythaemia (plethora), hypertension, gastritis, hepatitis, edoema, etc.,. Because it inhibits myocardial fibrosis, inflammation, and platelet aggregation, CH, an isoquinoline alkaloid, provides protection against myocardial ischemia injury. In the western world, acute myocardial infarction (AMI) is mostly caused by inflammation and fibrosis. Such a situation is improved by CH treatment.[22] Liensinine is an isoquinoline alkaloid that is isolated from the seed embryo of "Nelumbo Nucifera Gaertn," a plant having a wide range of biological activity. Liensinine has anti-pulmonary fibrosis, anti-hypertension, and other characteristics. Both Neferine and Liensinine have anticancer properties. Neferine prevents acute leukaemia cells from proliferating.[23]

1.5. COMPUTER AIDED DRUG DESIGN (CADD)

The level of structural knowledge and other details about the target (enzyme/receptor/protein) and the ligands that are available affect computer-aided drug design (CADD).[24] The basis of CADD involves theoretical approach based on molecular mechanics, quantum mechanics, molecular dynamics, structure-based drug design (SBDD), ligand-based drug design (LBDD), homology modeling, ligplot analysis, molecular docking, de novo drug design, pharmacophore modeling and mapping, virtual screening (VS), quantitative structure- activity relationships (QSARs)[25], In silico ADMET[26] (absorption, distribution, metabolism, excretion and toxicity) prediction etc.,. CADD centre was developed to foster collaborative research among biologist, biophysicists, structural biologists and computational scientists. The

primary objective of the CADD centre is to launch these collaborations that result in the formation of research projects to find novel chemical entities with the potential to be developed into novel therapeutic agents. There are few peers in the commercial sector for the lengthy, difficult, expensive, and extremely risky procedure that goes into discovering new drugs. For this reason, procedures for computer-aided drug design (CADD) are frequently applied in the pharmaceutical sector to shorten the procedure. Using computational tools during the lead optimization stage of drug development provides a significant economic benefit. A drug is typically introduced to the market after 10 to 15 years and between $500 and $800 million, with lead analogue production and testing accounting for a large segment of those costs. To cover a wide chemical space while minimising the number of compounds that must be synthesised and tested in vitro, computational tools in hit-to-lead optimization are advantageous. The premise underlying computational methods to drug design is that pharmacologically active compounds interact with their macromolecular targets, primarily proteins or nucleic acids, to exert their biological effects. Surfaces of molecules, electrostatic force, hydrophobic interaction, and hydrogen bond formation are important contributors to these interactions. These variables are mostly taken into account while analysing and predicting the interaction of two molecules.

A product is designed using computer technology known as computer-aided drug design, which also documents the design process. By transmitting precise schematics of a product's components, procedures, tolerances, and dimensions along with the right conventions for the product in question, CADD can streamline the production process.[27] It can be used to create two or three-dimensional diagrams that can be rotated to be seen from any angle, including from the inside looking out. Disease selection, target selection, lead compound identification, lead optimization, pre-

clinical trial testing, clinical trial testing, and pharmacogenomic optimization are the seven fundamental processes that make up the drug development process from idea to market. The final five steps must consistently pass in practice. Test compounds can be synthesised chemically or from natural sources (plants, animals, and microbes). Due to lack of efficiency, poor activity, toxicity, carcinogenicity, complexity of synthesis, insufficient efficiency, etc., these compounds may be disregarded as potentials. Only one of the 100,000 researched compounds may be released onto the market as a result, and the average cost of developing a new drug has increased to $800,000,000. Due to the high governmental standards for its execution, it is doubtful that the final steps of drug testing will take less time or incur a lower cost. Therefore, the stages of ligand identification and optimization are the focus of major efforts to increase drug development efficiency.[28] Through the use of bioinformatics tools, in silico methods can assist in discovering drug targets. They can also be used to generate candidate molecules, assess their similarity, dock these molecules with the target, rank them according to their binding affinities, and further optimise the molecule to improve binding affinities. They can also be used to analyse the target structure for potential binding/active sites. Computers and computational approaches are now used in every area of drug discovery, and they are the foundation for: (a) structure-based drug design and (b) ligand-based drug design.[29]

1.5.1. STRUCTURE-BASED DRUG DESIGN (SBDD):

The method to be applied in drug design is structure-based drug design. The development of novel drugs is aided by structure-based drug design.[30] The following elements make up the structure-based drug design process:

a) The chosen target should be prepared in solution form, and its structure should be determined with the aid of a Crystallography
b) To identify the binding site, the structure should be properly analysed
c) It is necessary to dock different compounds from databases at the binding site and then rank them according to their site affinity
d) Selected compounds are those that have the strongest affinity towards the site
e) Application of Leads and Tests that are designed to bind at the target sites is a component of biochemical tests
    I. If the lead is discovered to be acting as an inhibitor at the site, crystallography should be used to analyse its structure
    II. It should undergo additional potency and bioavailability testing before being launched
    III. Higher success rates can be achieved by modifying or optimising the action of the leads in Structure-Based Drug Design

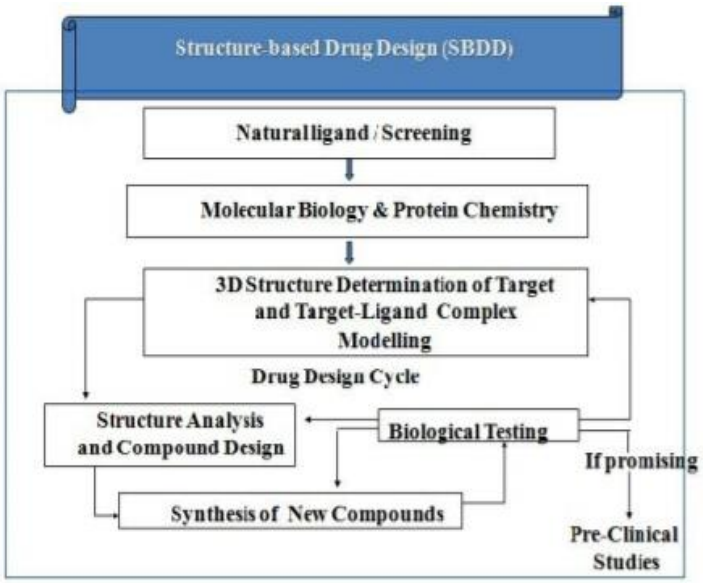

Figure 5: Structure based drug design

1.5.2. LIGAND- BASED DRUG DESIGN (LBDD)

Analysing ligands that are known to interact with a target is a component of the ligand-based drug discovery strategy. These techniques analyse the 2D or 3D structure of a set of reference compounds that are known to interact with the target of interest.[31] Drug design can sometimes be based on a procedure that uses the known ligands of a target protein as the starting point, typically when data pertaining to the 3D structure of a target protein are not accessible. The term "ligand-based drug design" refers to this strategy.[32]

a) Understanding molecules that bind to the intended target site is necessary for ligand-based drug design
b) To derive a pharmacophore model, these molecules could be employed
c) A molecule with the required structural capabilities to bind to a desired target site is known as a pharmacophore model

d) Once the pharmacophore is found, it is tested to see if the receptor will accept it; if not, the pharmacophore is further modified to become a potential drug

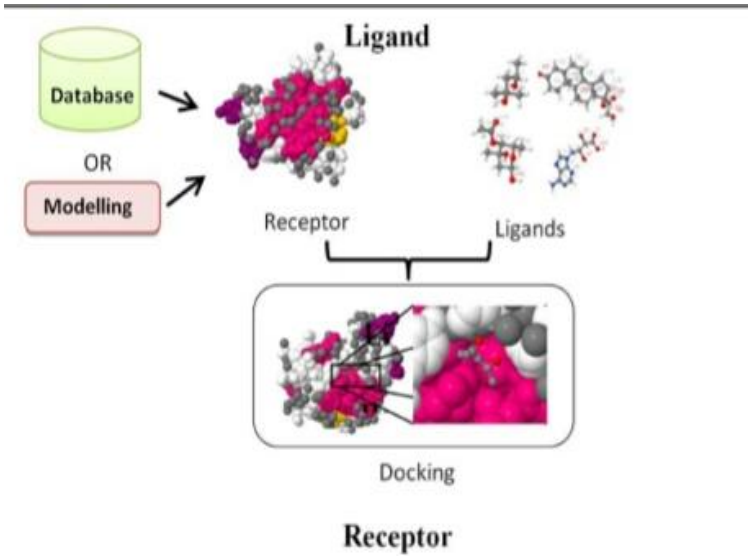

Figure 6: Ligand based drug design

Benefits of CADD

Cost savings: To reduce costs, many biopharmaceutical companies use CADD. CADD has replaced traditional experimentation that required using human and animal models, which saves cost and time. It is envisaged that computational drug design will play a significant role in lowering the likelihood of drug resistance in the case of specific diseases like influenza and, as a result, would lead to the manufacture of lead compounds that would target the causative factor. By utilising computational techniques, potent hits can be attained within a few weeks. The development of top-notch libraries and datasets that can be optimised for high molecular diversity or similarity is another benefit of CADD.

Limitations in CADD

The advancement of CADD is limited by the absence of reliable experimental data. It takes a while to complete some computer-aided drug design processes, especially when hunting for the appropriate lead component.

1.6. MOLECULAR DOCKING

An increasingly crucial tool for drug discovery is molecular docking. There is also discussion of the performance variations among the docking software options. The present docking methods have difficulty dealing with flexible receptor molecular docking approaches, particularly those that incorporate flexible receptor backbones. A recently created Local Move Monte Carlo (LMMC) based strategy is presented as a potential remedy for issues with flexible receptor docking. Molecular docking techniques for drug discovery are used in three application examples. There are increasingly more new therapeutic targets available for drug discovery as a result of the completion of the human genome project. Nuclear magnetic resonance spectroscopy, crystallography, and high-throughput protein purification methods have all been developed at the same time and have helped to unveil numerous structural details of proteins and protein-ligand complexes.[33]

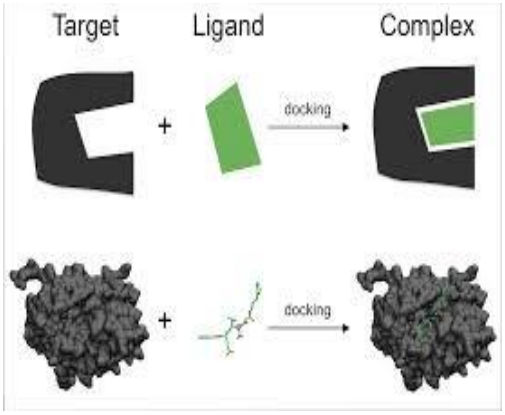

Figure 7: Schematic diagram of molecular docking

Today, all facets of drug development can be influenced by computational strategies, such as lead optimization tools and virtual screening (VS) procedures for hit detection. VS is a more direct and logical approach to drug discovery than conventional experimental high-throughput screening (HTS), and it has the advantage of being both inexpensive and effective screening. The two types of VS are ligand-based and structure-based methods. The use of ligand-based approaches, such as pharmacophore modelling and quantitative structure activity relationship (QSAR) methodologies, is possible when a set of active ligand molecules is known and little to no structural information about targets is available. The most popular approach for structure-based drug design is molecular docking, which has been in use since the early 1980s. Docking has become a more crucial tool in pharmaceutical research as a result of programmes based on various algorithms being created to perform molecular docking studies. Numerous great reviews on docking have previously been published, and numerous comparative studies have been carried out to assess the programmes' relative performance. We can define the behaviour of small molecules at the binding site of target proteins and understand basic biochemical processes by using the molecular docking approach to model the interaction between a small molecule and a protein at the atomic level. Prediction of the ligand conformation as well as its placement and orientation within these sites (often referred to as pose) and assessment of the binding affinity are the two fundamental steps in the docking process. These two actions have an impact on sample techniques and scoring systems, which will be covered in the theory section. The efficiency of docking procedures is greatly improved by knowing the location of the binding site prior to docking processes. Before docking ligands into the binding site, the binding site is frequently known. Additionally, by contrasting the target protein with a family of proteins that perform

a similar function or with proteins that have been co-crystallized with different ligands, one can learn additional information about the sites. Cavity detection programs or online servers, such as GRID, POCKET, Surf Net, PASS, and MMC, can be utilized to find putative active sites within proteins in the absence of knowledge about the binding sites. Blind docking is the process of docking without making any assumptions about the binding site. The lock-and-key theory proposed by Fischer, in which the ligand fits into the receptor like a lock and key, is an early explanation for the ligand-receptor binding mechanism. This notion served as the foundation for the earliest known docking techniques, which considered the ligand and receptor as rigid bodies. The "induced-fit" theory put out by Koshland then advances the "lock-and-key" theory by asserting that interactions between ligands and proteins constantly reshape the protein's active site. According to this theory, while docking, the ligand and receptor should be treated as flexible. As a result, it might better capture the binding events than the rigid treatment.

Since computer resources are limited, docking has been carried out with a flexible ligand and a rigid receptor for a long time and is still the most widely used technique. Although there have recently been numerous attempts to cope with receptor flexibility, flexible receptor docking, particularly backbone flexibility in receptors, still poses a significant difficulty for the available docking methods. In our research, we suggest a Local Move Monte Carlo (LMMC) method as a viable remedy for issues with flexible receptor docking.

1.6.1. Theory of docking

Using computational approaches, molecular docking essentially aims to anticipate the structure of the ligand-receptor complex. In order to perform docking, two interrelated steps must be taken: first, the ligand's conformations in the protein's active site must be sampled; next, these conformations must be ranked using a scoring function. The experimental binding mode should ideally be reproducible by sampling algorithms, and it should also be given the best rank among all created conformations. Here, we provide a succinct introduction of basic docking theory from these two perspectives. The modelling of two molecules interacting is a complex task. The intermolecular association is mediated by a variety of forces, including electrostatic, hydrogen-bonding, van der Waals, and stacking interactions between aromatic amino acids. Due to the complexity of the intermolecular interactions in a ligand-protein complex and the incomplete understanding of how the solvent affects the binding relationship, modelling these interactions is challenging. The lowest energy pathway is used to imitate the natural interaction between a ligand and its receptor during the docking process of a ligand to a binding site. It is easy to dock flexible ligands with rigid receptors and rigid ligands with rigid receptors, however it is problematic to use conventional docking methods when conformationally flexible ligands and receptors are involved. The optimal number of configurations that contain the experimentally discovered binding modes should be created by the search algorithm. Despite the fact that a thorough search algorithm would examine every potential mode of binding between the two molecules, this search would be impracticable due to the sheer size of the search space and the potential amount of time required to accomplish it. Since only a small portion of the entire conformational space can be sampled, it is necessary to strike a balance between the computational expense and the size of the search space

examined. Molecular dynamics, Monte Carlo methods, genetic algorithms, fragment-based, point complementary and distance geometry approaches, Tabu, and systematic searches are a few examples of popular search algorithms. The scoring function, on the other hand, comprises of many mathematical techniques that are used to predict the strength of the binding affinity, a non-covalent interaction. The development of an energy scoring function that can quickly and precisely characterise the interaction between the protein and ligand is a significant issue that affects all computational methodologies. The ligand contains a number of reviews about scoring. Rigid body docking and flexible docking are the two main components of the protein-ligand docking procedure.

Rigid Docking: The ligand and receptor are both treated as rigid entities in this approximation, which explores only six degrees of translational and rotational freedom and so completely rules out any flexibility. Rigid body docking procedure is the first step used by the majority of docking suite.

Flexible Docking: A technique that is more popular is to model the flexibility of the ligand while assuming that the protein receptor is rigid, focusing only on the conformational space of the ligand in the process. However, it is ideal to additionally take into account the flexibility of proteins, and some techniques in this regard have been established. To tackle ligand flexibility, algorithms fall into three broad categories: systematic methods, stochastic or random methods, and simulation methods.[10] The flexibility of proteins may be the most difficult problem in molecular docking because of their vast size and numerous degrees of freedom. Protein flexibility can be addressed using a variety of techniques, including soft docking, side-chain flexibility, molecular relaxation, and protein ensemble docking.

1.6.2. Experimental docking procedures

Numerous studies comparing the effectiveness of various molecular docking tools have been published, and there are several excellent reviews of molecular docking methods. We will now go over the four-step procedure used in this study to conduct the molecular docking.

Target selection

Although nuclear magnetic resonance or X-ray crystallography, which may be obtained from PDB, should ideally be used to determine the target structure experimentally, docking has been used successfully in place of homology models or threading. A high-quality model is required. A validation software like Molprobity[11] can be used to test it. The model must next be created by taking the water molecules out of the cavity, stabilising charges, adding the residues that are lacking, and generating the side chains, all in accordance with the parameters that are available. Biologically active and in a stable state, the receptor should be at this position.

Ligand selection and preparation

Depending on the objective, different ligands will be used for docking. It can be retrieved from a number of databases, such as ZINC or/and PubChem, or it can be drawn using the Chemsketch tool.[34] Applying filters is frequently required to lower the number of molecules that need to be docked. The net charge, molecular weight, polar surface area, solubility, commercial viability, similarity thresholds, pharmacophores, synthetic accessibility, and absorption, distribution, metabolism, excretion, and toxicological properties are a few examples.

Docking

The ligand is docked onto the receptor at this point, and the interactions are examined. The scoring function produces a score based on the ideal ligand that was chosen.

Evaluating docking results

The root-mean-square deviation (RMSD) between the experimentally observed heavy-atom positions of the ligands and the one(s) anticipated by the algorithm is typically used to assess how well docking algorithms predict a ligand binding pose. Finding the ideal stance is made difficult by the system's flexibility. One key factor that affects the conformational search's efficiency is the number of degrees of freedom that are included.[35] When the RMSD is less than 2Å, it is typically considered to be a strong performance.

Docking software description

To evaluate and explain ligand-protein or protein-protein interactions, there are numerous algorithms available, and their variety is ever-growing. For docking approaches to be successful, speed and accuracy are essential components. Numerous algorithms have novel extensions that combine their fundamental methodologies with an emphasis on speed and maximum accuracy. AutoDock[36] DOCK, FlexX, GOLD, ICM, ADAM, DARWIN, DIVALI, and DockVision are some of the most prominent docking programs.

AIM AND SCOPE OF THE STUDY

JAK has been involved in many inflammatory and neoplatic disorders like Rheumatoid arthritis, Psoriasis, Ulcerative colitis, Crohn disease, Polycythaemia Vera, Myeloproliferative cancers, Primary and secondary Myelofibrosis; Acute Myeloid Leukaemia, Essential Thrombocythemia etc.,. MPN is accompanied by inflammation, Splenomegaly and Thrombosis. 25 ligands were selected to check JAK1, JAK2, JAK3 and TYK2 inhibition and docking was carried out computationally in order to identify the better inhibitors of Janus Kinase proteins which supress disorders related to mutations of Janus Kinase family proteins. Minimum the binding energy, better will be the inhibitor.

CHAPTER 2

REVIEW OF LITERATURE

The Janus kinases, often known as JAKs, are a family of intracellular tyrosine kinases that are crucial for the signalling of a variety of cytokines that have been linked to the pathogenesis of myeloproliferative disorders and autoimmune disorders. Enhanced JAK kinase activity is mostly seen in patients having above disorders caused by somatic mutations. In the last decades, academic groups and certain pharmaceutical companies developed a range of JAK inhibitors to treat the mutations.

P. Xu, P. Shen, B. Yu, X. Xu, R Ge, *et al*., in ʻJanus Kinases(JAKs) reported the efficient therapeutic targets of autoimmune disease and myeloproliferative disorders'. The phosphotyrosines in the phosphorylated tyrosine residues served as docking sites for cytoplasmic signal transducer and activator of transcription (STAT) proteins, which were phosphorylated by the JAKs upon recruitment to the receptor complex. JAKs were activated upon ligand-induced receptor homo- or heterodimerization, which resulted in the immediate phosphorylation of tyrosine residues. The dimerized, phosphorylated STAT proteins travel to the cellular nucleus where they function as transcription factors. The only approved small molecule kinase inhibitors for immunological indications worked by interfering with the JAK-STAT system.[37]

T Kisseleva, S Bhattacharya, J Braunstein, C.W Schindler in ʻSignaling through the JAK/STAT pathway, reported in recent advances and future challenges': The JAK/STAT pathway was discovered as a result of research into the mechanism of cytokine signalling. Members of the janus activated kinase (JAK) family of tyrosine kinases activated signal transducers and activators of transcription (STATs) after

cytokines connect to their corresponding receptors. Once turned on, they formed dimers, go into the nucleus, and controlled the expression of the target genes. Significant progress had made over the past few years in characterising the JAK/STAT signalling cascade, including the discovery of numerous STATs and regulatory proteins.[38]

Current medicinal chemistry research is focused on developing new, effective JAK inhibitors. Additionally, it is being investigated whether second-generation inhibitors with selectivity for JAKs are more effective. This Perspective provides a reference and justification for the development of novel and potent JAKs inhibitors by summarising the progress made in the discovery and development of JAKs inhibitors, including the potential binding site and approaches for identifying small-molecule inhibitors. Future therapeutic perspectives in autoimmune diseases and myeloproliferative disorders are also presented.[37]

Rong Chen, Xiaodan Shi, Luojan Wang in their article 'Essential thrombocythemia with CALR mutation and recurrent stroke reported two case reports and literature review' says that some Essential thrombocythemia (ET) patients exhibit nonspecific symptoms and stroke events. Nonspecific features include head ache, visual disturbances, dysesthesia etc. It is important to pay attention to platelet count of patients with stroke and to identify type of gene mutation in patients with stroke and ET. New stroke in ET with CALR mutation has rarely been reported individualized therapy strategies specific to different gene mutation will be a relief for patients with ET and stroke.[39]

Yoko Edahiro in his article 'Treatment options and pregnancy management for patients with PV and ET' suggested that low-dose Aspirin and Phlebotomy are

favourable for patients with PV. Cytoreductive therapy is recommended for patients with high-risk PV. Same strategies are used to prevent thrombosis. As a treatment beyond JAK inhibitors; IFN is one of the most promising treatment options for PV or ET. Hydroxyurea is contraindicated during pregnancy. Several new agents such as HDAC inhibitor, LSD1 inhibitor, MDM2 inhibitors and hepcidin mimetics are used in addition to JAK2 inhibitors.[40]

Hui Shuai, Maksym Myronovskyi, Birgit Rosenkranzer, Constanze Paulus, Suvd Nadmid, Marc Stierhof, Dominik Kolling and Andriy Luzhetskyy in their article named 'Novel biosynthetic route to the Isoquinoline scaffold' explained a wide range of bioactivities like antitumor, antileukemic and anti-inflammatory properties of isoquinoline alkaloids. This project focuses on effect of isoquinoline alkaloids; ie, isoquinoline fused bicycles on treating JAK mutation disorders.[41]

H Ye, L Wang, L Ma, M Ionov, G Qiao, J Huang, L Cheng, Y Zhang, X Yang, S Cao in their article named 'Protein kinases as therapeutic targets to develop anticancer drugs with natural alkaloids' revealed an important class of natural compounds with a wide range of biological functions are alkaloids. Numerous alkaloids with considerable anticancer action through the inhibition of protein kinases have been discovered in past decades. The key enzymes that alkaloids target, such as mitogen-activated protein kinase (MAPK), phosphoinositide 3-kinase/protein kinase B/mammalian target of rapamycin (PI3K/AKT/mTOR), and janus-activated kinases/signal transducer and activator of transcription (JAK/STAT), will be discussed in the current mini-review. We will also highlight the difficulty and potential of creating alkaloids as novel anticancer drugs are also highlighted.[42]

CHAPTER 3

MATERIALS AND METHODS

The binding energy of the selected ligands to the proteins **3EYG**, **3FUP**, **5LWM**, and **4GJ2** was assessed using software. The following tools are employed and function as follows;

3.1 Marvin Sketch

Chemistry is translated into a digital environment utilizing Marvin Sketch. It has a large selection of features that make it possible to quickly and accurately sketch chemical compounds, reactions, Markush structures, and query molecules. Charge and polarizability, protonation and PK a, log P and log D, conformation and molecular dynamics, 3D alignment, topology, surface area, Huckel analysis (HOMO, LUMO, localization energy), and H-bond donor or acceptor properties. Additionally, Marvin Sketch features integrated property calculators that can obtain real-time information at your request, along with built-in structural and valence checkers that can offer guidance.

3.2. Maestro

Maestro is a critical component of the transformative drug discovery platform. It is used to optimise the design-make-test-analyse cycle, which produces higher-quality compounds faster. It models and interpret molecular interactions that aid in molecular design. Structural visualization is made possible since it’s a stream lined portal. It helps in target validation and structure enablement, Hit Discovery, Lead optimization.

3.3. Protein Data Bank

The Protein Data Bank (PDB) was established at Brookhaven National Laboratories (BNL) (1) in 1971 as an archive for biological macromolecular crystal structures. In 1980s number of deposited structures dramatically increased due to improvement in technology in crystallographic process, increase of structures determined by NMR methods, and changes in society views about data sharing. PDB is a database for 3D structural data of large biological molecule such as proteins and nucleic acids. It gives three-dimensional data of macromolecular structures that can be determined by Electron microscopy and X-ray crystallographic methods.

3.4. DOCKING

3.4.1 Biovia Discovery Studio

BIOVIA Discovery Studio brings together over 30 years of peer-reviewed research and world class insilico techniques such as molecular mechanics, free energy calculations, bio therapeutics develop ability and more into a common environment. It provides researchers with a complete toolset to explore the nuances of protein chemistry and catalyse discovery of small and large molecule therapeutics from Target ID to Lead Optimization.[41] Discovery Studio is a suitable software for stimulating small molecule and macro molecule system. Discovery Studio efficiently guides biological activities like anti-inflammatory activity, anti-tubercular activity, anti-bacterial activity, anti-viral activity, anti-diabetic and anti-oxidant activity.[41] Modelling tools in Biovia are designed to interpret complex data from X ray experiments. To quickly assign topology and parameter with high accuracy, Discovery Studio uses XPROLIG typing engine.

3.4.2. Auto dock

A collection of automated docking tools is called Auto Dock. It is intended to forecast how small molecules, such as substrates or drug candidates, would bind to a receptor with a known 3D structure. Auto Dock 4 and Auto Dock Vina are the two software generations that make up the current distributions of Auto Dock. In reality, Auto Dock 4 consists of two primary programmes: Auto dock, that performs the docking of the ligand to a set of grids that describe the target protein; these grids are precalculated by auto grid. Atomic affinity grids can be visualised in addition to being used for docking. This might, for instance, assist organic synthetic chemists develop better binders. In Auto Dock Vina, it is not necessary to choose atom types and precalculated grid maps for them. Instead, it internally calculates the grids for the required atom types, and it does it virtually instantly.

3.4.3. Cygwin

Cygwin is free software that provides a Unix-like environment and software tool set to users of any modern x86 32-bit and 64-bit versions of MS-Windows.

3.4.4. Ligand Structures

The structures of the twenty-five ligands used for docking are given below,

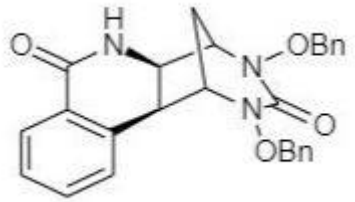

Ligand 1

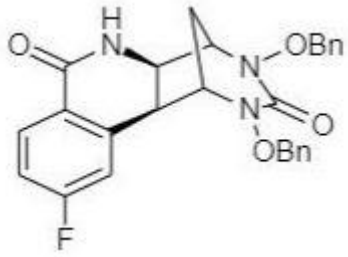

Ligand 2

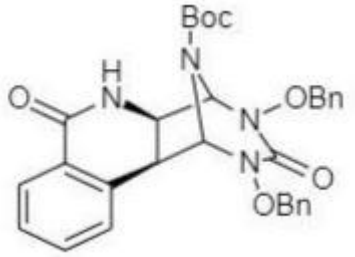

Ligand 3

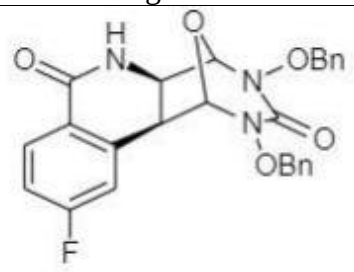

Ligand 4

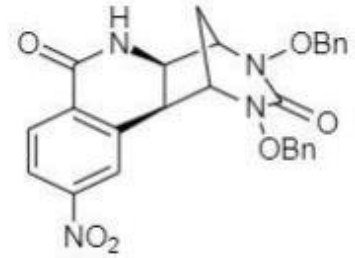

Ligand 5

Ligand 6

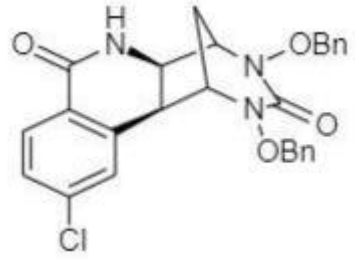

Ligand 7

Ligand 8

Ligand 9

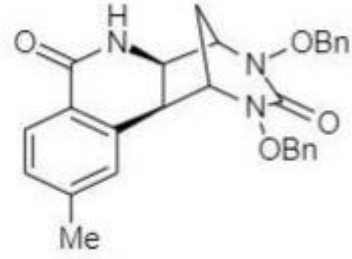

Ligand 10

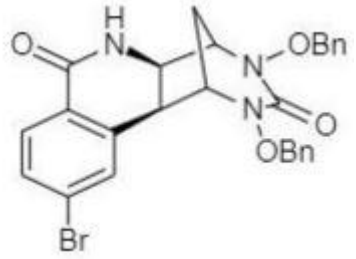 Ligand 11	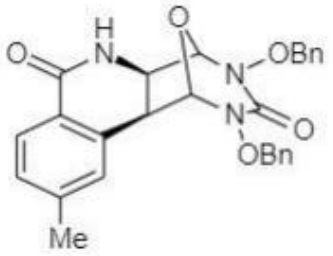 Ligand 12
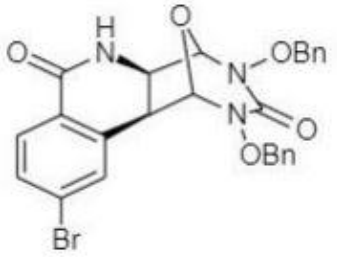 Ligand 13	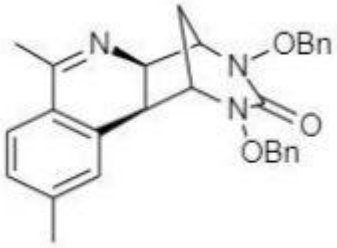 Ligand 14
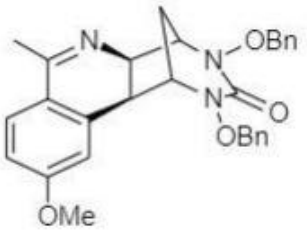 Ligand 15	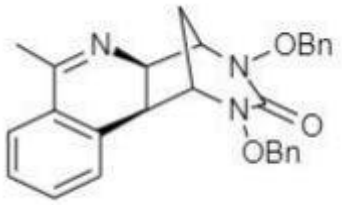 Ligand 16
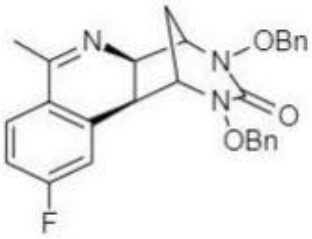 Ligand 17	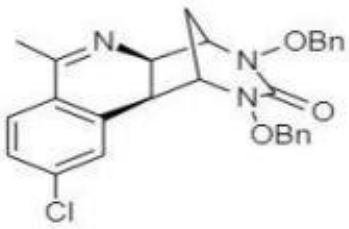 Ligand 18
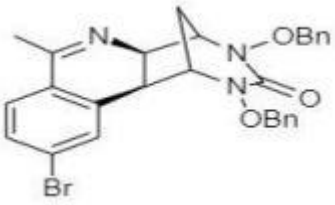 Ligand 19	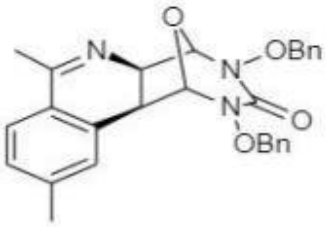 Ligand 20
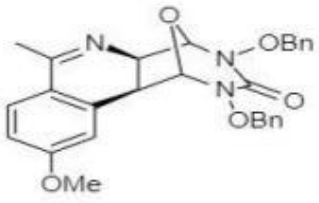 Ligand 21	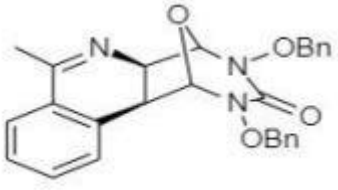 Ligand 22

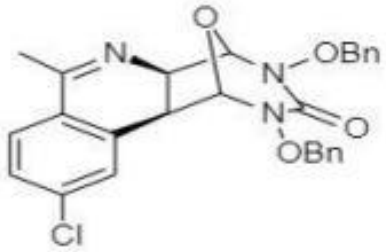 Ligand 23	 Ligand 24
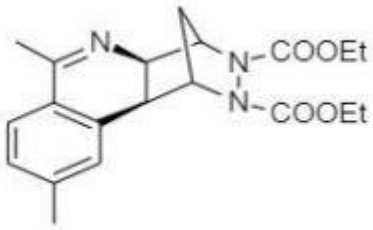 Ligand 25	

Table 1: Structure of ligands

3.5. Structure of protein

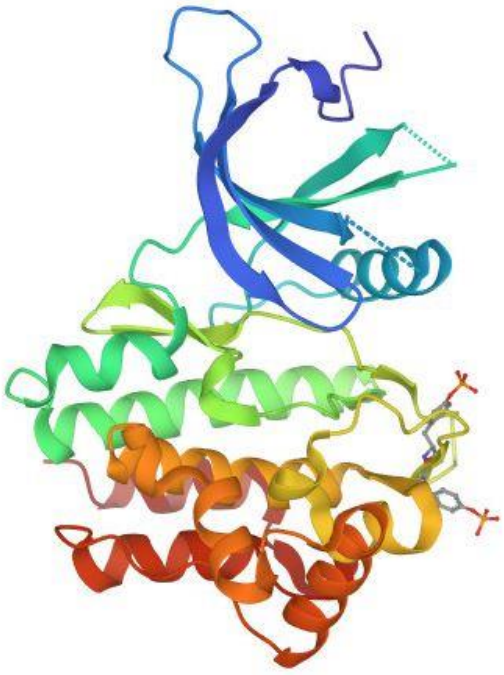

Figure 8: 3EYG protein

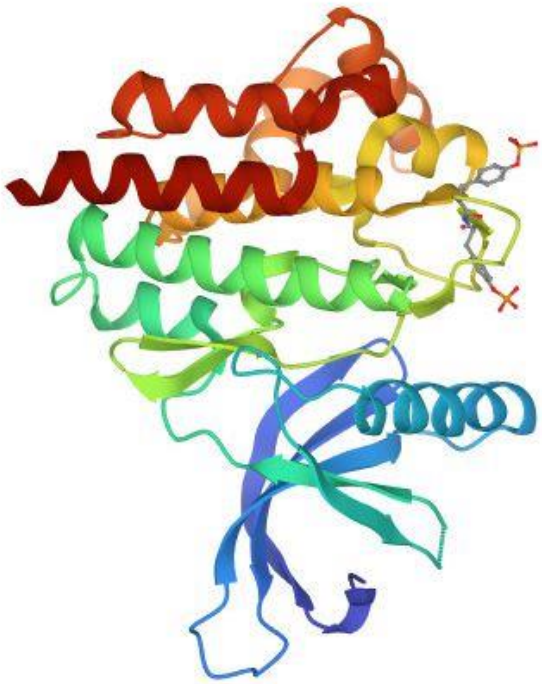

Figure 9: 3FUP protein

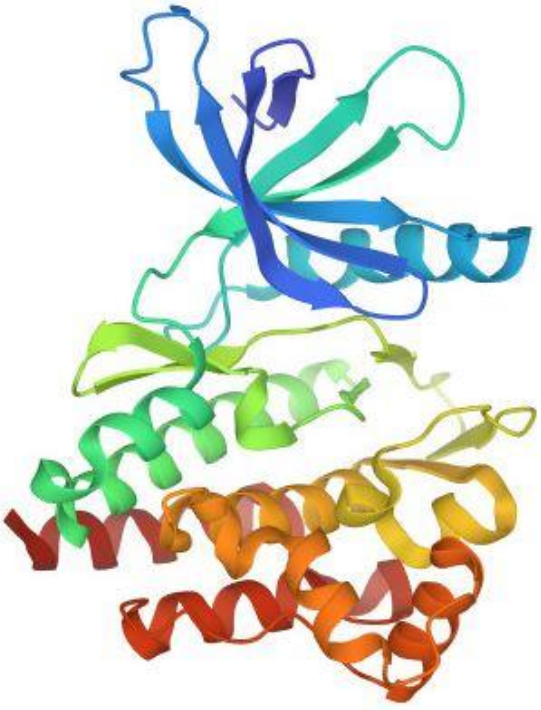

Figure 10: 5LWM protein

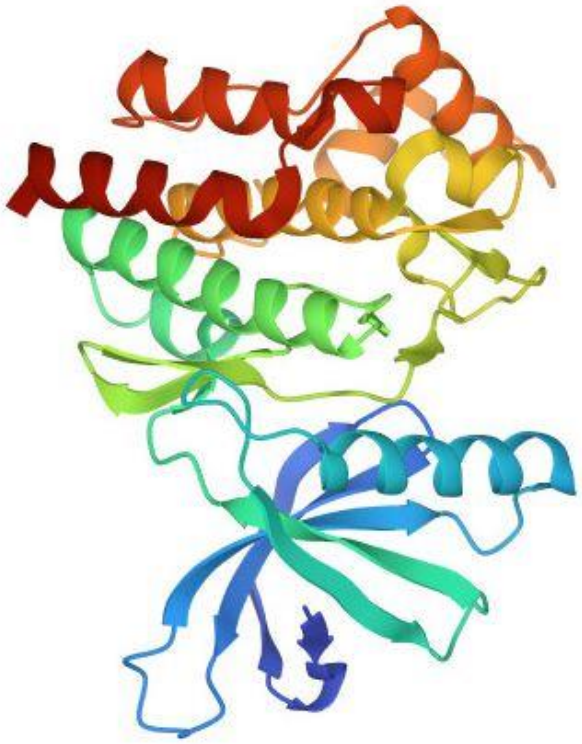

Figure 11: 4GJ2 protein

3.6. Methodology

Proteins associated with JAK1, JAK2, JAK3, TYK2, 3EYG, 3FUP, 5LWM and 4GJ2 respectively was retrieved from protein data bank. The protein was downloaded in PDB format. Then using Maestro12.3 the protein was splitted into ligand, water etc and the ligand and protein are saved as .pdb format. This protein was cleaned in Discovery Studio and all hetero atoms and unwanted ligands were deleted in this and saved as protein .ppd .pdb. the above saved protein .ppd is converted into .pdbqt. Similarly, our ligands (given structure) which was drawn using Marvin Sketch are cleaned in 2D and then in 3D. Both the protein and ligands were saved in pdbqt format using Autodock. The active site residue for; JAK1 is taken as LEU959, JAK2 is taken as 3FUP, JAK3 is taken as 5LWM and TYK2 is taken as 4GJ2 which are selected by reading various research papers. The grid box was generated with coordinates (12.19,

6.174, -14.1) for JAK1, (-52.062, 13.174, 3.951) for JAK2, (31.76, 21.248, 49.128) for JAK3, (-10.71, -5.525, -15.767) for TYK2 with dimensions 60 x 60 x 60 Å. Then are saved as .gpf format. Similarly docking is done with 50 Genetic algorithm runs and saved in .dpf format. Using Cygwin the commands were given and docking was completed for 50 runs. 2D interaction diagram was observed for further investigations.

CHAPTER 4

RESULT AND DISCUSSION

Molecular Docking was carried out using software AutoDock. **3EYG**, **3FUP**, **5LWM** and **4GJ2** proteins of JAK1, JAK2, JAK3 and TYK2 were selected respectively. 50 selected ligands were used for docking process. In docking active site of proteins were blocked by using the set of ligands. Blocking will inhibit cell growth and cell division. Auto Dock provide more information about binding energy in which ligand perfectly fit to protein. The binding energy obtained with Auto Dock software is given in **table 2**.

From this table it is evident that different ligands have different binding energy with respect to respective Janus Kinase proteins.

Ligand Name	**Binding Energy Associated with JAK1 protein**	**Binding Energy Associated with JAK2 protein**	**Binding Energy Associated with JAK3 protein**	**Binding Energy Associated with TYK2 protein**
Ligand 1	-9.93	-10.66	-10.51	-9.64
Ligand 2	-9.86	-10.49	-10.19	-9.37
Ligand 3	-9.84	-10.45	-10.19	-9.76
Ligand 4	-9.93	-10.33	-10.02	-9.53
Ligand 5	-10.98	-10.53	-10.92	-10.55
Ligand 6	-9.63	-10.11	-10.60	-9.88
Ligand 7	-9.81	-10.83	-9.97	-10.34
Ligand 8	-9.49	-9.66	-10.50	-9.67
Ligand 9	-9.69	-10.71	-10.38	-10.08
Ligand 10	-10.02	-10.69	-10.08	-10.23
Ligand 11	-10.01	-11.08	-9.90	**-10.66**
Ligand 12	-9.99	-10.80	-10.30	-9.86
Ligand 13	-10.31	-11.07	-10-67	-10.26
Ligand 14	-10.53	-10.14	-10.94	-10.01
Ligand 15	**-11.39**	**-11.63**	-10.93	-9.98
Ligand 16	-10.03	-10.22	-10.32	-9.56
Ligand 17	-9.85	-10.27	-10.31	-9.33
Ligand 18	-10.75	-10.74	-10.37	-10.22
Ligand 19	-10.86	-10.65	-10.78	-10.41
Ligand 20	-10.03	-10.26	-10.18	-9.76
Ligand 21	-10.30	-10.05	**-11.19**	-9.50
Ligand 22	-9.90	-10.27	-9.93	-9.57
Ligand 23	-10.32	-10.52	-10.24	-10.01
Ligand 24	-10.75	-10.70	-10.18	-10.26
Ligand 25	-8.47	-8.46	-8.98	-8.20

Table 2 : Binding energy of ligands

Analysis of JAK1

Using Autodock calculations the highest negative binding energy value was observed for **ligand 15** (-11.39 kcal/mol) and hence maximum stability for docked complex. **Ligand 25** has the highest binding energy (-8.47kcal/mol) and hence minimum stability among the docked complexes.

Ligand 15 shows various interactions such as van der Waals, conventional hydrogen bond, carbon hydrogen bond, π-sigma, amide-π stacked, alkyl, π-alkyl interactions. Van der Waals interactions are shown by Lys888, Gly882, Arg1007, Gly962, Pro960, Phe958, Leu959, Glu957, Gly1020, Asp1021, Gly884, Gly887. Conventional hydrogen bond is exhibited by Ser963. Carbon hydrogen interaction is shown by Asn1008. Leu881 show π-sigma interaction. Glu883 show amide-π stacked interaction. Lys908, Val938, Ala906 shows alkyl interation and Leu1010, Val889, Met956 shows π-alkyl interactions. The amount of binding energy obtained for **ligand 15** is -11.39 kcal/mol.

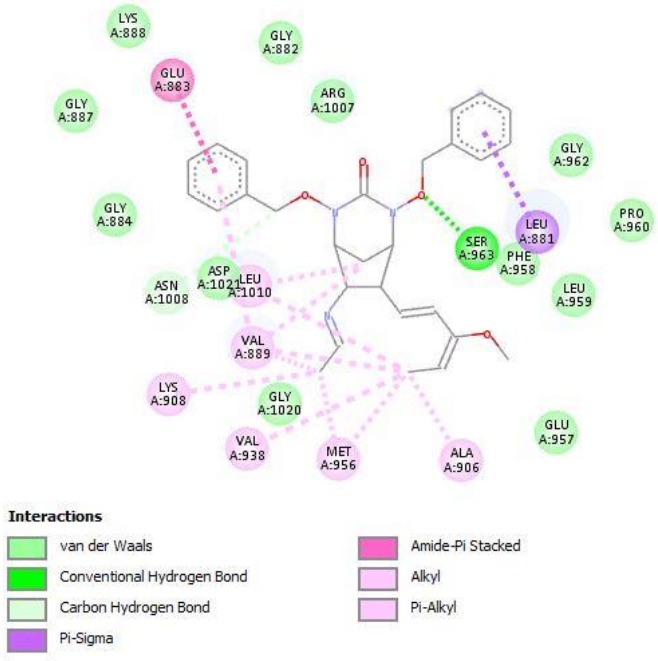

Figure 12: 2D interaction of protein with **ligand 15**

Ligand 25 shows van der Waals interaction with Glu957, Gly1020, Asp1021, Glu883, Glu966, Gly882, Ser963, Gly962. Lys908, Arg1007, Phe958, Ala906, Met956, Leu959, Val938, Leu1010, Val889, Leu881 shows alkyl and alkyl-π interactions. The amount of binding energy obtained is -8.47 kcal/mol. **Ligand 25** has the highest binding energy and hence minimum stability.

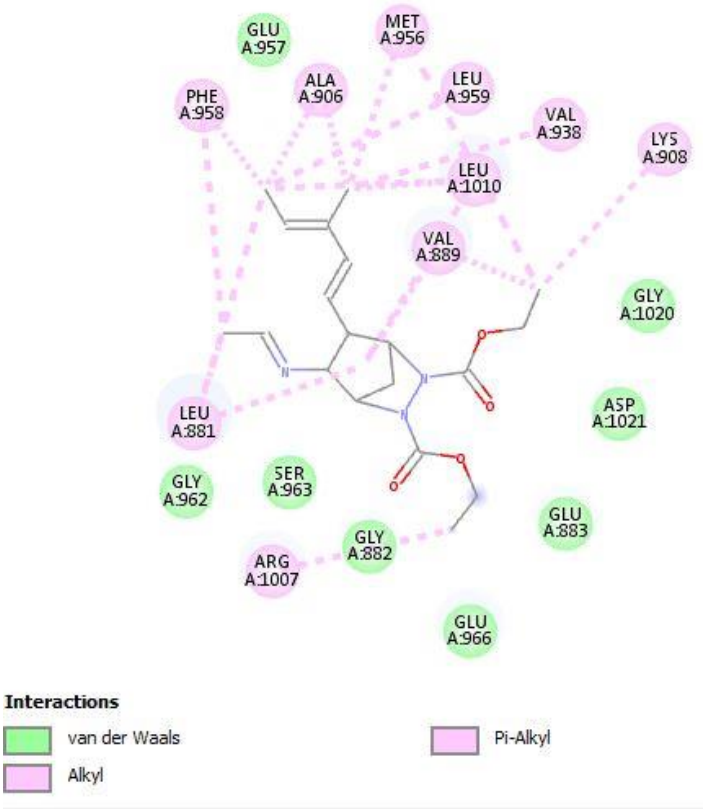

Figure 13: 2D interaction of protein with **ligand 25**

Of these 25 ligands which are docked to the protein, **ligand 15** showed more negative binding energy (-11.39 kcal/mol). On comparing the structures of the ligands, **ligand 2**, **5**, **6**, **7**, **10**, and **11** have the same scaffold structures with **ligand 1**, having different functional groups attached to **ligand 1** such as –F, -NO_2, -OMe, -Cl, -Me and -Br respectively. **Ligand 1** has a binding energy of -9.93 kcal/mol. **Ligands 2**, **5**, **6**, **7**, **10** and **11** have binding energies -9.86, -10.98, -9.63, -9.81, -10.02, -10.01 kcal/mol respectively. Among these, **ligand 5** which has electron withdrawing -NO_2 as

substituent has the most negative binding energy followed by **ligand 10** which has –Me as the substituent.

Ligand 3 has a binding energy of -9.84 kcal/mol. **Ligand 3** differs from **ligand 1** in having an oxygen atom at the bridge head. Thus, we see that the presence of oxygen atom on the bridge head increases the binding energy a little. **Ligand 4**, **8**, **9**, **12** and **13** have the same scaffold structure with **ligand 3**, having different functional groups attached such as –F, -OMe, -Cl, -Me, and –Br respectively. **Ligand 4**, **8**, **9**,**12** and **13** have binding energies -9.93, -9.49, -9.69, -9.99 and -10.31 kcal/mol respectively. Among these the **ligand 13** which has –Br as substituent has the most negative binding energy followed by **ligand 12** which has –Me as substituent.

Ligand 16 has a binding energy of -10.03 kcal/mol. **Ligand 14**, **15**, **17**, **18** and **19** have the same scaffold structures with **ligand 16**, having different functional groups attached to such as –Me, -OMe, -F, -Cl and-Br with binding energies -10.53, -11.39, -9.85, -10.75, -10.86 kcal/mol respectively. Among these, **ligand 15** with-OMe has the most negative binding energy followed by **ligand 19** with -Br atom.

Ligand 22 differs from **ligand 16** in having an oxygen atom at the bridge head. **Ligand 22** has binding energy of –9.90 kcal/mol which is a little higher when compared with **ligand 16**. **Ligand 20**, **21**, **23** and **24** have the same scaffold structures with **ligand 22**, having different functional groups attached such as –Me, -OMe, -Cl and –Br with binding energies -10.03, - 10.30, -10.32 and -10.75 kcal/mol respectively. Among these, **ligand 24** with –Br substituent has the most negative binding energy.

Ligand 25 which has –COOEt substituent attached to it has the highest binding energy among all the ligands; -8.47 kcal/mol. Thus, having minimum stability.

Analysis of JAK2

Using Autodock calculations the highest negative binding energy value was observed for **ligand 15** (-11.63 kcal/mol) and hence maximum stability for docked complex. **Ligand 25** has the highest binding energy (-8.46kcal/mol) and hence minimum stability among the docked complexes.

Ligand 15 shows various interactions such as van der Waals, conventional hydrogen bonding, carbon hydrogen bonding, π-sigma, π-sulfur, amide-π stacked, alkyl and alykl-π interactions. Van der Waals interactions are shown by Arg980, Tyr932, Leu932, Glu930, Gly993, Ser862, Asp994, Gly856, Gly861, Gly858. Conventional hydrogen bonding is exhibited by Ser936. Carbon hydrogen bond is exhibited by Asn981. π-sulfur interaction is shown by Met929. π-sigma interaction is shown by Gly935, Leu983 and Leu855. Lys857 show amide-π stacked interaction. Alkyl and π-alkyl interactions are shown byVal863.Lys882, Val911, Ala880. The amount of binding energy obtained is -11.63 kcal/mol.

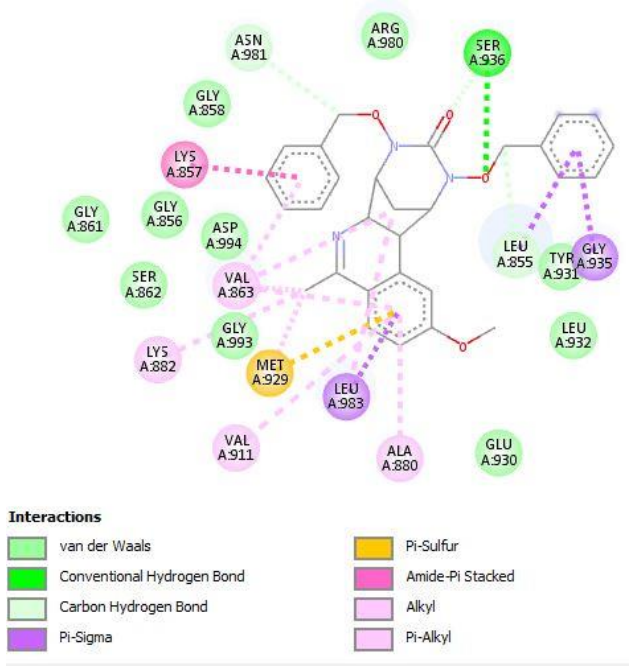

Figure 14: 2D interaction of protein with **ligand 15**

Ligand 25 shows van der Waals, carbon hydrogen, π-sigma, alkyl, π-alkyl interactions. Van der Waals interactions are shown by Ser936, Gly935, Leu932, Glu930, Lys882, Gly993, Asp994, Lys857, Arg938. Carbon hydrogen bond is shown by Asp939 and Gly856. π-sigma interaction is shown by Leu983 and Leu855. Tyr931, Ala880, Val911, Met929, Val863, Arg980 and Leu855 shows alkyl and alkyl-π interactions. The amount of binding energy is -8.46 kcal/mol. **Ligand 25** has the highest binding energy and hence minimum stability.

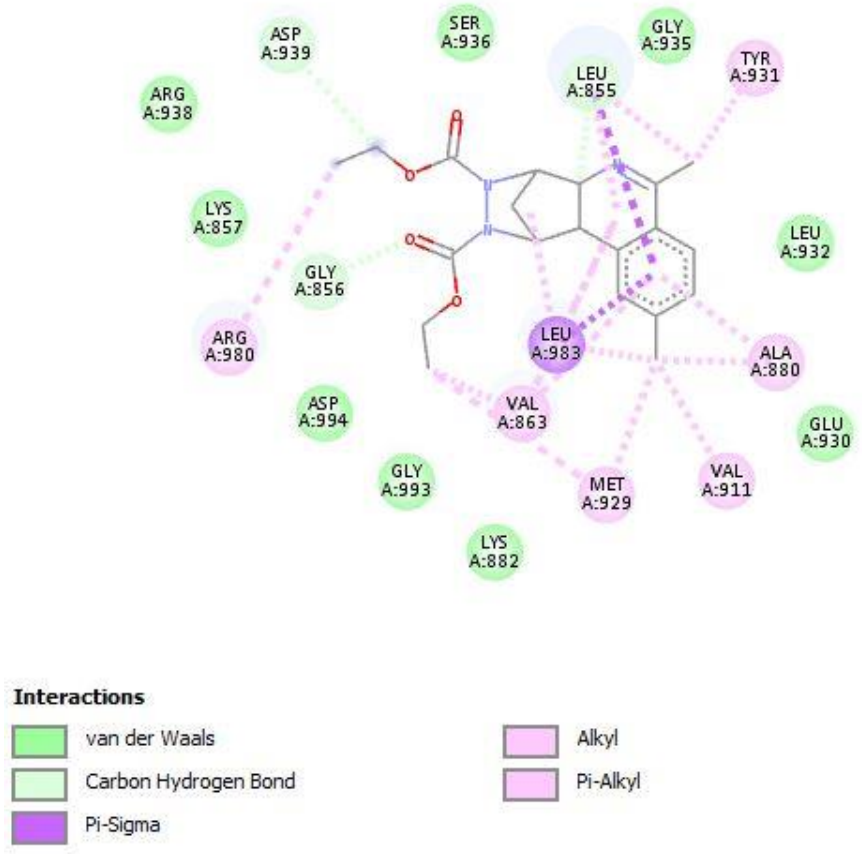

Figure 15: 2D interaction of protein with **ligand 25**

Of these 25 ligands which are docked to the protein, **ligand 15** showed more negative binding energy (-11.63 kcal/mol). On comparing the structures of the ligands, **ligand 2**, **5**, **6**, **7**, **10**, and **11** have the same scaffold structures with **ligand 1**, having different functional groups attached to **ligand 1** such as –F, -NO_2, -OMe, -Cl, -Me and -Br

respectively. **Ligand 1** has a binding energy of -10.66 kcal/mol. **Ligand 2**, **5**, **6**, **7**, **10** and **11** have binding energies -10.49, -10.53, -10.11, -10.83, -10.69, -11.08 kcal/mol respectively. Among these, **ligand 11** which has –Br as substituent has the most negative binding energy followed by **ligand 7** which has –Cl as the substituent.

Ligand 3 has a binding energy of -10.45 kcal/mol. **Ligand 3** differs from **ligand 1** in having an oxygen atom at the bridge head. Thus, we see that the presence of oxygen atom on the bridge head increases the binding energy a little. **Ligand 4**, **8**, **9**, **12** and **13** have the same scaffold structure with **ligand 3**, having different functional groups attached such as –F, -OMe, -Cl, -Me, and –Br respectively. **Ligand 4**, **8**, **9**,**12** and **13** have binding energies -10.33, -9.66, -10.71, -10.80 and -11.07 kcal/mol respectively. Among these, the **ligand 13** which has –Br as substituent has the most negative binding energy followed by **ligand 12** which has –Me as substituent.

Ligand 16 has a binding energy of -10.22 kcal/mol. **Ligand 14**, **15**, **17**, **18** and **19** have the same scaffold structures with **ligand 16**, having different functional groups attached to such as –Me, -OMe, -F, -Cl and-Br with binding energies -10.14, -11.63, -10.27, -10.74, -10.65 kcal/mol respectively. Among these, **ligand 15** with-OMe has the most negative binding energy followed by **ligand 18** with -Cl atom.

Ligand 22 differs from **ligand 16** in having an oxygen atom at the bridge head. **Ligand 22** has binding energy of –10.27 kcal/mol which is a little lower when compared with **ligand 16**. **Ligand 20**, **21**, **23** and **24** have the same scaffold structures with **ligand 22**, having different functional groups attached such as –Me, -OMe, -Cl and –Br with binding energies -10.26, - 10.05, -10.52 and -10.70 kcal/mol respectively. Among these, **ligand 24** with –Br substituent has the most negative binding energy.

Ligand 25 which has –COOEt substituent attached to it has the highest binding energy among all the ligands, -8.46 kcal/mol. Thus, having minimum stability.

Analysis of JAK3

Using Autodock calculations the highest negative binding energy value was observed for **ligand 21** (-11.19 kcal/mol) and hence maximum stability for docked complex. **Ligand 25** has the highest binding energy (-8.98kcal/mol) and hence minimum stability among the docked complexes.

In **ligand 21** van der Waals interaction is shown by Leu875, Glu871, Leu900, Ala853, Leu905, Pro906, Gly908, Cys909, Lys830, Gly829, Ser835, Gly831, Asn954, Arg953 and Gly834. Conventional hydrogen bond interaction is shown byAsp967. Phe968 and Glu903 shows carbon hydrogen bond and π-donor hydrogen bond interaction. π-sigma interaction is shown by Val836 and Leu956. Met902 shows π-sulfur interaction. Alkyl and π-alkyl interaction is shown by Val884, Ala966, Leu828, Tyr904, Leu956 and Lys855. The amount of binding energy obtained is -11.19 kcal/mol.

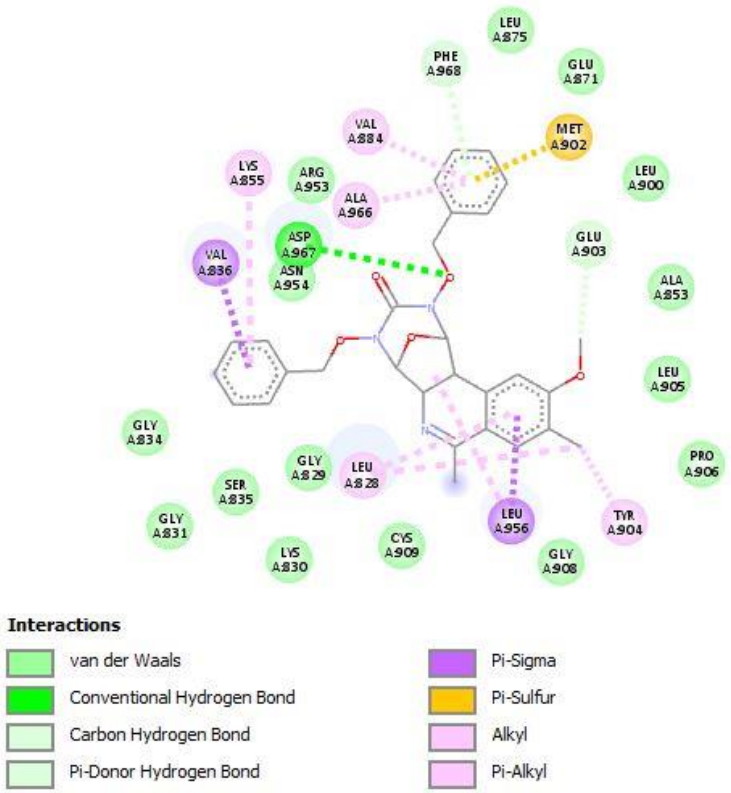

Figure 16: 2D interaction of protein with **ligand 21**

Ligand 25 shows van der Waals interactions with Asn954, Arg953, Asp967, Phe968, Glu871, Glu903, Pro906 and Gly908. Leu905 shows coventional hydrogen bonding interactions. π-sigma bond interaction is shown by Val836. Met902 shows π-sulfur interaction. Leu828, Ala853, Lys855, Ala966, Leu956, Val884, Tyr904 shows alkyl and alkyl-π interactions. The amount of binding energy obtained is -8.98 kcal/mol. **Ligand 25** has the highest binding energy and hence minimum stability. The high binding energy is due to the presence of unfavourable bump which interacts with various aminoacids.

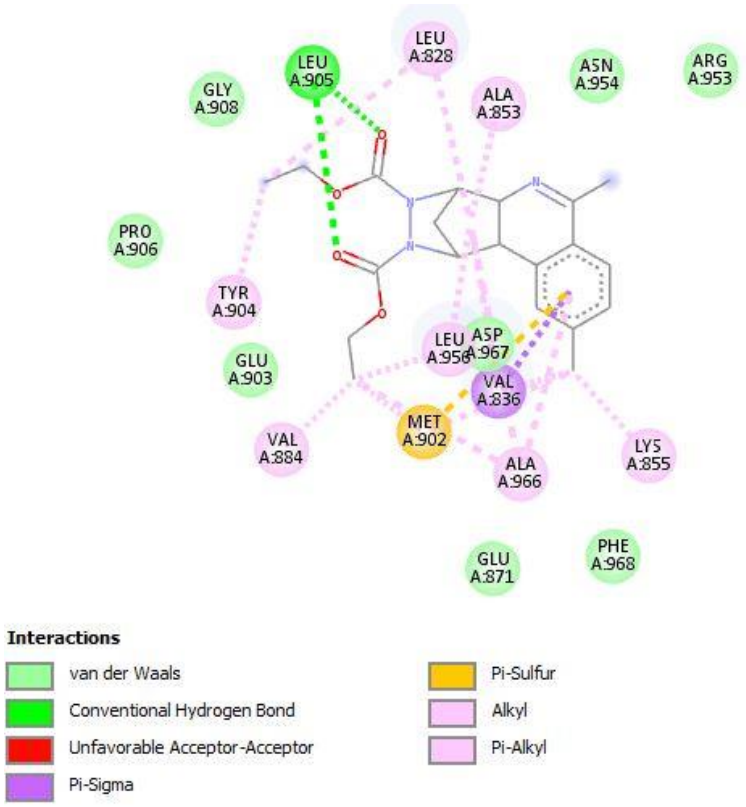

Figure 17: 2D interaction of protein with **ligand 25**

Of these 25 ligands which are docked to the protein, **ligand 21** showed more negative binding energy (-11.19 kcal/mol). On comparing the structures of the ligands, **ligand 2**, **5**, **6**, **7**, **10**, and **11** have the same scaffold structures with **ligand 1**, having different functional groups attached to **ligand 1** such as –F, -NO_2, -OMe, -Cl, -Me and -Br respectively. **Ligand 1** has a binding energy of -10.51 kcal/mol. **Ligand 2**, **5**, **6**, **7**, **10** and **11** have binding energies -10.19, -10.92, -10.60, -9.97, -10.08, -9.90 kcal/mol respectively. Among these, **ligand 5** which has –NO_2 as substituent has the most negative binding energy followed by **ligand 6** which has –OMe as the substituent.

Ligand 3 has a binding energy of -10.19 kcal/mol. **Ligand 3** differs from **ligand 1** in having an oxygen atom at the bridge head. Thus, we see that the presence of oxygen atom on the bridge head increases the binding energy a little. **Ligand 4**, **8**, **9**, **12** and

13 have the same scaffold structure with **ligand 3**, having different functional groups attached such as –F, -OMe, -Cl, -Me, and –Br respectively. **Ligand 4**, **8**, **9**, **12** and **13** have binding energies -10.02, -10.50, -10.38, -10.30 and -10.67 kcal/mol respectively. Among these, the **ligand 13** which has –Br as substituent has the most negative binding energy followed by **ligand 8** which has –OMe as substituent.

Ligand 16 has a binding energy of -10.32 kcal/mol. **Ligand 14**, **15**, **17**, **18** and **19** have the same scaffold structures with **ligand 16**, having different functional groups attached to such as –Me, -OMe, -F, -Cl and-Br with binding energies -10.94, -10.93, -10.31, -10.37, -10.78 kcal/mol respectively. Among these, **ligand 14** with –Me has the most negative binding energy followed by **ligand 15** with –OMe group.

Ligand 22 differs from **ligand 16** in having an oxygen atom at the bridge head. **Ligand 22** has binding energy of –9.93 kcal/mol which is higher when compared with **ligand 16**. **Ligand 20**, **21**, **23** and **24** have the same scaffold structures with **ligand 22**, having different functional groups attached such as –Me, -OMe, -Cl and –Br with binding energies -10.18, - 11.19, -10.24 and -10.18 kcal/mol respectively. Among these, **ligand 21** with –OMe substituent has the most negative binding energy.

Ligand 25 which has –COOEt substituent attached to it has the highest binding energy among all the ligands; -8.98 kcal/mol. Thus, having minimum stability.

Analysis of TYK2

Using Autodock calculations the highest negative binding energy value was observed for **ligand 11** (-10.66 kcal/mol) and hence maximum stability for docked complex. **Ligand 25** has the highest binding energy (-8.20 kcal/mol) and hence minimum stability among the docked complexes.

Ligand 11 shows van der Waals interactions with Lys930, Gly1040, Glu979, Tyr980, Gly984, Ser985, Gly904, Asn1023, His907, Arg1027, Gly906, Asp1041 and Glu905. Carbon hydrogen bond interaction is shown by Asn1028. π-sigma interaction by Val911 and π-sulfur by Met978. Alkyl and alkyl-π interactions are shown by Val911, Ile960, Leu1030, Ala928, Val981 and Leu903. The amount of binding energy obtained is -10.66 kcal/mol.

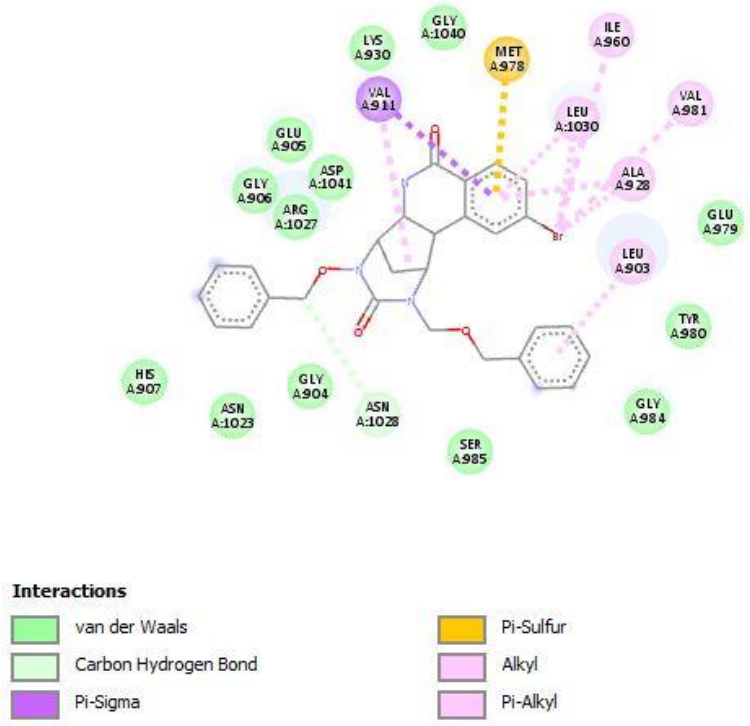

Figure 18 : 2D interaction of protein with **ligand 11**

Ligand 25 shows van der Waals interactions with Glu905, Gly904, Asp988, Ser985, Gly984, Glu979, Gly1040 and Asp1041.Lys930 exhibits conventional hydrogen bond interaction. Glu906 and Asn1028 shows carbon hydrogen bond interaction. π-sigma interactions are exhibited by Leu903 and Leu1030. Alkyl and alkyl-π interactions are shown by Val911, Leu903, Leu1030, Val981, Tyr980, Ala928, Ile960, Met978 and Arg1027. The amount of binding energy obtained is -8.20 kcal/mol. **Ligand 25** has the highest binding energy and hence minimum stability.

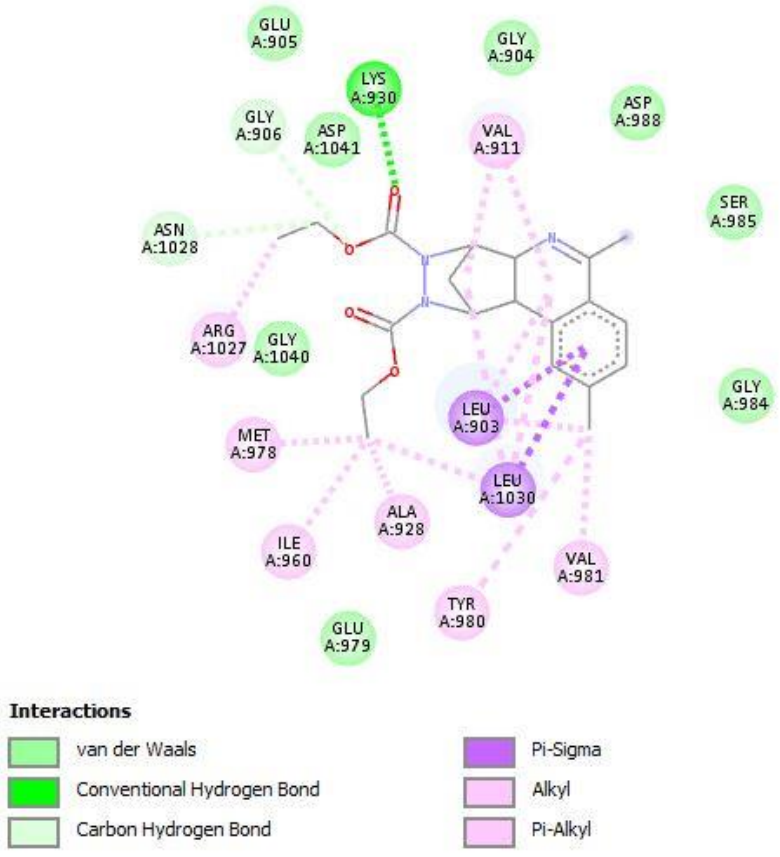

Figure 19: 2D interaction of protein with **ligand 25**

Of these 25 ligands which are docked to the protein, **ligand 11** showed more negative binding energy (-10.66 kcal/mol). On comparing the structures of the ligands, **ligand 2**, **5**, **6**, **7**, **10**, and **11** have the same scaffold structures with **ligand 1**, having different functional groups attached to **ligand 1** such as –F, -NO_2, -OMe, -Cl, -Me and -Br

respectively. **Ligand 1** has a binding energy of -9.64 kcal/mol. **Ligands 2**, **5**, **6**, **7**, **10** and **11** have binding energies -9.34, -10.55, -9.88, -10.34, -10.23, -10.66 kcal/mol respectively. Among these, **ligand 11** which has –Br as substituent has the most negative binding energy followed by **ligand 5** which has $–NO_2$ as the substituent.

Ligand 3 has a binding energy of -9.76 kcal/mol. **Ligand 3** differs from **ligand 1** in having an oxygen atom at the bridge head. Thus, we see that the presence of oxygen atom on the bridge head decreases the binding energy a little here. **Ligand 4**, **8**, **9**, **12** and **13** have the same scaffold structure with **ligand 3**, having different functional groups attached such as –F, -OMe, -Cl, -Me, and –Br respectively. **Ligand 4**, **8**, **9**,**12** and **13** have binding energies -9.53, -9.67, -10.08, -9.86 and -10.26 kcal/mol respectively. Among these the **ligand 13** which has –Br as substituent has the most negative binding energy followed by **ligand 9** which has –Cl as substituent.

Ligand 16 has a binding energy of -9.56 kcal/mol. **Ligand 14**, **15**, **17**, **18** and **19** have the same scaffold structures with **ligand 16**, having different functional groups attached to such as –Me, -OMe, -F, -Cl and-Br with binding energies -10.01, -9.98, -9.33, -10.22, -10.41 kcal/mol respectively. Among these, **ligand 19** with –Br has the most negative binding energy followed by **ligand 18** with –Cl atom.

Ligand 22 differs from **ligand 16** in having an oxygen atom at the bridge head. **Ligand 22** has binding energy of –9.57 kcal/mol which is a little lower when compared with **ligand 16**. **Ligand 20**, **21**, **23** and **24** have the same scaffold structures with **ligand 22**, having different functional groups attached such as –Me, -OMe, -Cl and –Br with binding energies -9.76, - 9.50, -10.01 and -10.26 kcal/mol respectively. Among these, **ligand 24** with –Br substituent has the most negative binding energy.

Ligand 25 which has –COOEt substituent attached to it has the highest binding energy among all the ligands; -8.20 kcal/mol. Thus, having minimum stability.

CHAPTER 5

CONCLUSION

The study of molecular docking using Auto Dock, conducted to **JAK1**, **JAK2**, **JAK3** and **TYK2** proteins of Janus Kinase family proteins using isoquinoline fused bicycles are provided. Lower the binding energy, greater its affinity to bind with protein. Different ligand shows different binding energies due to the presence of various functional groups. While analysing ligands of similar scaffold and different substituents attached, least negative binding energy is shown by ligands having highly electronegative 'F' attached to it. Other electronegative elements like Cl, Br attached ligands show more negative binding energies compared to above one. Ligands free of substituents also show least negative binding energy. When bulky groups like $-CO_2Et$ attached to ligands, they show more negative binding energy. Ligands having five membered substituent also poses more negative binding energy. In case of docking on **JAK1**, **ligand 15** got more negative binding energy or least binding energy (-11.39 kcal/mol), docking on **JAK2**, **ligand 15** got least binding energy (-11.63 kcal/mol), docking on **JAK3**, **ligand 21** showed the least binding energy (-11.19 kcal/mol) and docking on **TYK2** showed that, **ligand 20** has least binding energy (-10.66 kcal/mol).

REFERENCES

1. Gadina M., Hilton D., Johnston JA., Morinobu A., Lighvani A., Zhaou YJ., Visconti R., O´shea JJ (**2001**), Singnaling by type I and II cytokine receptors:ten years after, *Curr.Opin.Immunol.*,13(3): 363-373. doi:10.1016/S0952-7915(00)00228-4

2. R. RoskoskiJr (**2016**), Janus kinase (JAK) inhibitors in the treatment of inflammatory and neoplastic diseases, *Pharmacological Research.* 111, 784-803. https://doi.org/10.1016/j.phrs.2016.07.038

3. Nordqvist C. (**2011**)., Protein JAK Makes Cancer Cells Contract., *Medicinal News Today.*

4. Tefferi A. (**2010**). Novel mutations and their functional and clinical relevance in myeloproliferative neoplasms: JAK2, MPL, TET2, ASXL1, CBL, IDH and IKZF1. *Leukemia*, 24(6), 1128–1138. https://doi.org/10.1038/leu.2010.69

5. Kumar N., Kuang L., Villa R., Kumar P., Mishra J. (**2021**), Mucosal Epithelial Jak Kinases in Health and Diseases. *Mediators of Inflammation.*1-17.

6. Mishra J, Karanki SS, Kumar N (**2012**). Identification of molecular switch regulating interactions of Janus Kinase 3 with cytoskeletal proteins. *The Journal of Biological Chemistry.* 287 (49): 41386–91. doi:10.1074/jbc.C112.363507

7. Mishra J, Waters CM, Kumar N (**2012**). Molecular mechanism of interleukin-2-induced mucosal homeostasis. *American Journal of Physiology. Cell Physiology*. 302 (5): C735-47.

8. Kumar N, Mishra J, Narang VS, Waters CM (**2007**). Janus kinase 3regulates interleukin 2-induced mucosal wound repair through tyrosine phosphorylation of villin. *The Journal of Biological Chemistry*. 282(42): 30341–5. doi:10.1074/jbc.C600319200

9. Leonard WJ, O'Shea JJ (**1998**). Jaks and STATs: biological implications. *Annual Review of Immunology.* 16: 293–322. doi:10.1146/annurev.immunol.16.1.293
10. Johnston JA, Kawamura M, Kirken RA, Chen YQ, Blake TB, Shibuya K, Ortaldo JR, McVicar DW, O'Shea JJ (**1994**). Phosphorylation and activation of Jak-3 Janus Kinase in response to interleukin-2. *Nature.* 370 (6485): 151–3. doi:10.1038/370151a0
11. Krolewski JJ, Lee R, Eddy R, Shows TB, Dalla-Favera R (**1990**). Identification and chromosomal mapping of new human tyrosine kinase genes. *Oncogene.* 5 (3): 277–82.
12. Stark GR, Kerr IM, Williams BR, Silverman RH, Schreiber RD (**1998**).How cells responds to interferons. *Annu. Rev. Biochem*. 67 (1): 227–64.
13. Shaw MH, Freeman GJ, Scott MF, Fox BA, Bzik DJ, Belkaid Y, Yap GS. (**2006**). Tyk2 negatively regulates adaptive Th1 immunity by mediating IL-10 signaling and promoting IFN-γ-dependent IL-10 reactivation. *J. Immunol*. 176 (12): 7263–71. doi:10.4049/jimmunol.176.12.7263
14. P.J. Lupardus, M. Ultsch, H. Wallweber, P. Bir Kohli, A.R. Johnson, C. Eigenbrot, Structure of the pseudokinase-kinase domains from protein kinase TYK2 reveals a mechanism for Janus kinase (JAK) autoinhibition, *Proc. Natl. Acad. Sci. U. S. A.* 111 (**2014**) 8025–8030.
15. Kontzias A, Kotlyar A, Laurence A, Changelian P, O'Shea JJ (**2012**). Jaknibs: a new clss of kinase inhibitors in cancer and autoimmune disease. *Current Opinion in Pharmacology*. 12 (4): 464–70
16. Pesu M, Laurence A, Kishore N, Zwillich SH, Chan G, O'Shea JJ (**2008**). Therapeutic targeting of Janus Kinase. *Immunological Reviews*. 223: 132–42.

17. Norman P (**2014**). Selective JAK inhibitors in development for rheumatoid arthritis. *Expert Opinion on Investigational Drugs*. 23 (8): 1067–77.
18. JAK Inhibitors Showing Promise for Many Skin Problems - Conditions ranging from alopecia to vitiligo. (**2017**).
19. Forster M, Gehringer M, Laufer SA (**2017**). Recent advances in JAK3 inhibition: Isoform selectivity by covalent cysteine targeting. *Bioorganic & Medicinal Chemistry Letters.* 27 (18): 4229–4237.
20. Furumoto Y, Gadina M (**2013**). The arrival of JAK inhibitors: advancing the treatment of immune and hematologic disorders. *BioDrugs*. 27 (5): 431–8.
21. Shang, X. F., Yang, C. J., Morris-Natschke, S. L., Li, J. C., Yin, X. D., Liu, Y. Q., Guo, X., Peng, J. W., Goto, M., Zhang, J. Y., & Lee, K. H. (**2020**). Biologically active isoquinoline alkaloids covering 2014-2018. *Medicinal research reviews*, 40(6), 2212–2289. https://doi.org/10.1002/med.21703
22. Bai, R., Yin, X., Feng, X., Cao, Y., Wu, Y., Zhu, Z., Li, C., Tu, P., & Chai, X. (**2017**). Corydalis hendersonii Hemsl. protects against myocardial injury by attenuating inflammation and fibrosis via NF-κB and JAK2-STAT3 signaling pathways. *Journal of ethnopharmacology*, 207, 174-183
23. Zhou, J., Li, G., Zheng, Y., Shen, H. M., Hu, X., Ming, Q. L., Huang, C., Li, P., & Gao, N. (**2015**). A novel autophagy/mitophagy inhibitor liensinine sensitizes breast cancer cells to chemotherapy through DNM1L-mediated mitochondrial fission. *Autophagy*, 11(8),1259–1279. https://doi.org/10.1080/15548627.2015.1056970
24. Sehgal, V. K.; Das, S.; Vardhan, A. (**2007**) computer aided drug designing, DOI:10.19056/ijmdsjssmes/2017/v6i1/125571
25. Borman, S.;(**1990**) New QSAR Techniques Eyed for Environmental Assessments, *Chem Eng News* 68:20-3

26. Anderson, A. C.; (**2003**) The process of Structure Based Drug Design. *J Chembiol*; 10:7 87- 97

27. Yun T, Weiliang Z, Kaixian C, Hualiang J(**2006**). New technologies in computer-aided drug design: Toward target identification and new chemical entity discovery. *Drug discovery today: technologies*. 3 (3), 307-313.

28. Pranita, P. K.; Madhavi, M. M.; Rishikesh, V. A.; Rajesh, J. O.; Sandip, S. K. (**2012**) Computer-aided drug design: an innovative tool for modelling. *Journal of medicinal chemistry*. 2, 139 -148

29. Pugazhendhi, D.; Umamaheswari, T. S. (**2013**) In silico methods in drug discovery–a review; 46 *International journal of advanced research in computer science and software engineering*; 3 (5); 680-683.

30. http://www.slideshare.net/adammbbs/structure-based-drug-design-48389641/12; Structure-based drug design (Docking and de novo drug design); Authored by Adam Shahul Hameed; Anna University Chennai; Available online from **2015**

31. Satyajit, D.; Sovan, S.; Kapil, S.(**2010**). Computer-aided drug design - a new approach in drug design and discover. 4(3), 146-151

32. Choudhary, L. K.; Shukla, A.; Zade, S.; Charde, R.(**2011**). (C.A.D.D.)-a new modern software- based approach in drug design and discovery;*International journal of pharmaceutical chemistry*, 1(1) 10-20.

33. Nataraj S. P., Khajamohiddin S., Tuszynski J.(**2017**) Software for molecular docking, *Biophysical reviews* 9 (2), 91-102

34. Garrett M. M.; Margueritta L W.(**2008**) Molecular docking, *molecular modelling of proteins*, 365-382

35. Meng X., zhang. H, Mezei. M, Cui M (**2011**). Molecular docking: a powerful approach for structure-based drug discovery, *current computer aided drug design* 7 (2), 146-157

36. Arcon.J P., Modenutti.C P, Avendaño D., Lopez E D., Defelipe L A, Ambrosio F A, Turjanski A G, Forli S, Marti M A (**2019**). Autodock Bias: improving binding mode prediction and virtual screening using known protein-ligand interactions, *Bioinformatics* 35 (19), 3836-3838.

37. Xu P; Shen P; Yu B; Xu X; Ge R; Cheng X; Chen Q; Bian J; Li Z; Wang J (**2020**). Janus kinases (JAKs): The efficient therapeutic targets for autoimmune diseases and myeloproliferative disorders. *European Journal of Medicinal Chemistry*, 112155–.

38. Kisseleva T, Bhattacharya S, Braunstein J, Schindler C W (**2002**). Signaling through the JAK/STAT pathway, recent advances and future challenges.*Gene* 285 (1-2), 1-24.

39. Chen R, Shi X, Wang L, Wang X, Wei J, Kang X, Du F, Gao S, Yang F, Jiang W (**2022**). Essential thromocythemia with CALR mutation and recurrent stroke: two case reports and literature review. *Therapeutic advances in neurological disorders*. 15(1).

40. Edahiro Y (**2022**). Treatment options and pregnancy management. *International Journal of Hematology*. 115, 659-671

41. Shuai H, Myronovskyi M, Rosenkranzer B, Paulus C, Nadmid S, Stierhof M, Kolling D, Luzhetskyy A (**2022**) Novel biosynthetic route to the Isoquinoline scaffold. *American Chemical Society*. 17(3), 598-608.

42. Ye H, Wang L, Ma L, Ionov M, Qiao G, Huang J, Cheng L, Zhang Y, Yang X, Cao S (**2021**). Protein kinases as therapeutic targets to develop anticancer drugs with natural alkaloids. *Front. Biosci*. 26(11), 1349-1361.

****